

# NUMERICAL MODELING OF FORMATION INVASION

YALCHIN EFENDIEV\*

**Abstract.** In this work we consider the formation invasion. During the drilling processes rotary drilling fluid invades the wellbore and creates the mudcake in the wellbore and invades the reservoir. In this work we numerically model this processes.

## 1. Introduction

The first oil well in the United States was drilled with cable tools in 1859 to a depth of 56 feet. This was the historic Drake well located near Titusville, Pennsylvania. It is credit with having started the American petroleum industry. The cable tools are believed to have been employed first by the early Chinese in the drilling of brine wells.

The rotary drilling method is comparatively new, and first practiced by Leschot, a French engineer in 1863. United States patents on rotary equipment were issued around 1866. Nowadays the rotary drilling method is widely used. In the rotary method, the hole is drilled by a rotating bit to which a downward force is applied. The bit is fastened to a drill string, composed of high quality drill pipe and drill collars, with new sections being added as drilling progresses. The cuttings are lifted from the hole by the drilling fluid which is continuously circulated down the inside of the drill string through water courses or nozzles in the bit, and upward in the annular space between the drill pipe and the bore hole. At the surface, the returning fluid is diverted through a series of tanks which afford a sufficient period to allow cutting separation and any necessary treating. In the last these pits the mud is picked by the pump suction and repeats the cycle.

Rotary drilling equipment is complex and any detailed discussion is above the scope of this work. The rotary drilling fluid is usually governed by the specific requirements of the geologic area. The great majority of the drilling fluids (muds) contain suspended solid particles in the fluid. Muds serve a numerical practical purposes. For example, they cool and lubricate the drill bit, remove and bring the cuttings to the surface, and importantly provide increased hydrostatic pressure for well control.

During the drilling processes, the drill bit exposes the virgin formation to drilling mud. During initial times of the invasion phase the mud enters formation freely. Filtrating through the boundaries of the wellbore the solid particles of the mud deposit to the wellbore. This starts the process of the mudcake build-up. Once the internal cake forms and pore bridging stabilizes, the dominant role of external mudcake build-up becomes more apparent. As the drilling mud is forced into the formation under high pressure, its constituent solids left behind outside of the invaded rock. The mudcake starts thickening. As the internal cake is forming the water (assuming that the mud is water based) filtrates into the reservoir and displace the oil. This processes can be described using two phase flow model.

As the mudcake grows the presence of the annular flow becomes more important. The annular flow act as to erode the cake. In particular, under the shear stresses of the annular

---

\*Institute for Mathematics and Its Applications, Univeristy of Minnesota, Minneapolis, MN 55455

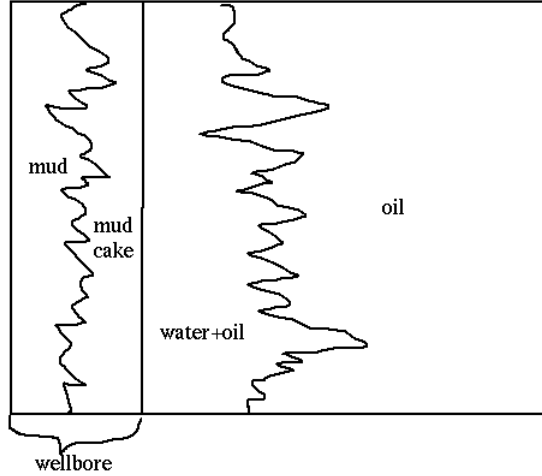


FIG. 2.1. A schematic plot of the invasion process

flow the mudcake starts eroding after some time. This happens when the gel stress of the mud cake becomes equal to the shear stresses of the annular flow. After this the growth of the mudcake reaches the equilibrium.

The fluid modeling is important because it forms the essentials of the log analysis. For any given resistivity logging instrument tool response is complex, and depends on the wave frequencies, formation properties, etc. The knowledge of formation properties allows the analysts to quantify the problem in some sense.

In this paper we consider the static filtration. In this case we can neglect the effects of the shear stresses and assume that the mud flow is horizontal.

The paper is organized in the following way. In section 2 we consider the equation for the mudcake growth and the equations for two-phase flow. The section 3 is devoted to the numerical results. Finally, in section 4 we draw conclusions.

## 2. Static filtration

We consider a vertical well. This allows us to consider only the cross sectional model assuming the radial symmetry along the horizontal direction. In Fig. 2.1 the mud cake formation and the invasion phenomena is schematically depicted.

### 2.1. The mud cake growth

To model the cake thickness  $x_c(t)$  (following [1]) we assume that the volume fraction of solid and liquid suspensions are constant and do not change in time. Denote  $V_s$  and  $V_l$  the volumes

of solid and liquids in the mud and  $f_s$  the solid fraction,

$$f_s = \frac{V_s}{V_s + V_l}.$$

Since the solid fraction does not change over the time we have the following conservation property:

$$dV_s = \frac{f_s}{1 - f_s} dV_l. \quad (2.1)$$

To define the mudcake thickness we note that the total volume of solids  $dV_s$  deposited on the elemental area  $dA$  during time  $dt$  is

$$dV_s = (1 - \phi_c) dA dx_c \quad (2.2)$$

where  $\phi_c$  is the porosity of the mud, and  $dx_c$  is the increase in the mud thickness. Note that the deposition rate of the solids is proportional to the porosity of the mud.

Furthermore we replace  $dV_s$  in (2.2) by  $dV_l$  based on (2.1):

$$dV_l \frac{f_s}{1 - f_s} = (1 - \phi_c) dA dx_c. \quad (2.3)$$

Because of the incompressibility  $dV_l$  can be expressed through the velocity,  $v_n$ , at the wellbore boundary in the following simple way (conservation of the liquid phase):

$$dV_l = v_n dA dt.$$

Substituting this expression into (2.3) we get

$$\frac{dx_c}{dt} = \frac{f_s}{(1 - f_s)(1 - \phi_c)} v_n. \quad (2.4)$$

This is the equation for the mud cake gross in the absence of shear stresses.

## 2.2. Invasion of the liquid into the reservoir

To model the invasion (filtration) of the liquid into the reservoir two-phase immiscible flow model will be used. To introduce two-phase immiscible flow model denote by  $\mu_w$  and  $\mu_o$  the viscosities of the water and oil,  $S_w$  and  $S_o$  the saturations of the water and oil,  $k$  the absolute permeability of the reservoir,  $k_{rw}$ ,  $k_{ro}$  the relative permeabilities of the water and oil phases,  $\rho_w$  and  $\rho_o$  the pressure for water and oil phases, and  $p_w$  and  $p_o$  the pressure for water and oil phases.

The velocity of each phase can be expressed through the permeability and the pressure of the phase using Darcy's law:

$$v_w^i = \frac{k^{ij}}{\mu_w} k_{rw} (\nabla_j p_w - \rho_w g e_z);$$

$$v_o^i = \frac{k^{ij}}{\mu_o} k_{ro} (\nabla_j p_o - \rho_o g e_z).$$

where  $v_w^i$  and  $v_o^i$  are the components of the water and oil phases,  $g$  is the gravitational constant and  $e_z$  is the unit vector in the vertical direction.

For our analysis we neglect the effects of gravity and capillary effects. The absence of the capillary effects gives us  $p_w = p_o$ . Then the total velocity becomes

$$v^i = v_w^i + v_o^i = k^{ij} \left( \frac{k_{rw}}{\mu_w} + \frac{k_{ro}}{\mu_o} \right) \nabla_j p.$$

The saturation of the water phase ( $S_w$ ;  $S_o = 1 - S_w$ ) satisfy the following conservation law:

$$\phi \frac{\partial S_w}{\partial t} + \nabla_i v_w^i = 0.$$

Next, we express  $v_w^i$  through the total velocity as

$$v_w^i = f v^i,$$

where

$$f = \frac{k_{rw}/\mu_w}{k_{rw}/\mu_w + k_{ro}/\mu_o}$$

Thus the final equations for twophase immiscible flow without the capillary and gravity effects are

$$\begin{aligned} \nabla_i k^{ij} \left( \frac{k_{rw}}{\mu_w} + \frac{k_{ro}}{\mu_o} \right) \nabla_j p &= 0 \\ \phi \frac{\partial S}{\partial t} + \nabla_i v^i f(S) &= 0. \end{aligned} \tag{2.5}$$

With the effects of gravity and capillary two phase immiscible flow satisfy:

$$\begin{aligned} \nabla_i k^{ij} \left( \frac{k_{rw}}{\mu_w} + \frac{k_{ro}}{\mu_o} \right) \nabla_j p_o &= 0 \\ v_i &= k^{ij} \left( \frac{k_{rw}}{\mu_w} + \frac{k_{ro}}{\mu_o} \right) \nabla_j p_o = 0 \\ \phi \frac{\partial S}{\partial t} + \nabla_i (v_i f(S)) - \epsilon \nabla_i D^{ij}(S, x) \nabla_j S + f(S) g_z k^{ij} k_{ro}(S) (\rho^o - \rho^w) e_z^j &= 0, \end{aligned} \tag{2.6}$$

where  $S$  stands for the saturation of the water phase, and  $p$  is so called hydrostatic pressure.

### 3. Numerical results

Denote the horizontal direction by  $x$ , the vertical direction by  $y$ ,  $x = x_{wb}$  the location of the wellbore which is fixed, and  $x_c(y)$  the thickness of the mudcake at the depth  $y$  we have the following final system of equation without the effects of gravity and capillary:

$$\begin{aligned} \nabla_i k^{ij} \left( \frac{k_{rw}}{\mu_w} + \frac{k_{ro}}{\mu_o} \right) \nabla_j p &= 0, \text{ if } x > x_{wb} \\ \phi \frac{\partial S}{\partial t} + \nabla_i v^i f(S) &= 0, \text{ if } x > x_{wb} \\ \nabla_i k^{ij} \nabla_j p &= 0, \text{ if } x < x_{wb} \\ \frac{dx_c(y)}{dt} &= \frac{f_s}{(1 - f_s)(1 - \phi_c)} v^2(x_{wb}, y). \end{aligned} \tag{3.1}$$

Here we assume that the mud flow in the wellbore between mudcake and the drilling pipe satisfy the Darcy's law. This assumption is true for the static filtration. Note that  $x > x_{wb}$  is the reservoir and  $x < x_{wb}$  is the wellbore. The third equation in the wellbore describes the flow in the mudcake and the flow between the drill pipe and the mudcake. Note that the permeability of the mudcake ( $[x_c, x_{wb}]$ ) is very small compare other permeabilities in the problem.

We apply finite volume procedure for the solution of pressure equation in the reservoir ( $x > x_{wb}$ ) and the solution of flow in the wellbore ( $x < x_{wb}$ ). For the solution of the saturation equation the second order TVD scheme is applied. For the numerical cells where only some part of the cell is occupied by the mudcake ( $k_{mud}$  being the permeability) and the other is by the Darcy flow ( $k$  being the permeability) we assign the permeability to these cells based on homogenization theory. According to these results the permeability in the horizontal direction is the harmonic average of the two permeabilities of  $k_{mud}$  and  $k$  and the permeability in the vertical direction is the arithmetic average of these two permeabilities.

To present the numerical results the following parameters we use the following parameters:

the pressure difference is 150 psi  
the viscosity of the water is 1 centipoise  
the viscosity of the oil is 5 centipoise  
the horizontal length of the interest (reservoir) 2 feet  
the vertical length of the drillpipe 50 feet  
the radius of the wellbore 0.2 ft  
the porosity of the reservoir 0.2  
the porosity of the mudcake 0.1  
the permeability of the mudcake 0.01 md

The permeability of the reservoir is assumed to be heterogeneous with log-normal distribution. The parameters of this random distribution are taken to be: correlation length in the horizontal direction 0.2; the correlation in the vertical direction 0.02; and the variance is 2.0. The mean value of the permeability is taken to be 10 mdarcy. The relative permeabilities are assumed to be  $k_{rw} = S_w^2$ ,  $k_{ro} = S_o^2$ .

The system of equations is solved using finite volume technique. Each time instant, first the pressure field in the reservoir are calculated solving the Darcy's law (elliptic), then the saturation field in the filtrated area are updated. The finite volume technique assures the conservation property of the system.

In the following examples the effects of the capillarity pressure and the gravity have been neglected. In the Figure 3.1, the plots on the right side are the saturation fronts and the corresponding plots on the left side are the mudcake. The wellbore boundary is assumed to be at  $x = 0$ , the drill is at  $x = -0.4$ . For example the plot for the mudcake (left plots) shows that everything right of the curves is mudcake while left of this curve is the mud. As we see as the time evolves the thickness of the mudcake grows (or the curve moves towards right). Similarly in the contour plots for the saturation field the left from the contour lines is the untouched oil while contour lines show the mixture of the oil an water behind the front. In Fig. 3.2 we change the pressure drop to be 100 psi. In this case the invasion process is slower compare to the previous case. In Fig. 3.3 we plot the mudcake curve in a limited distance interval to show the heterogeneity of the moving mudcake front.

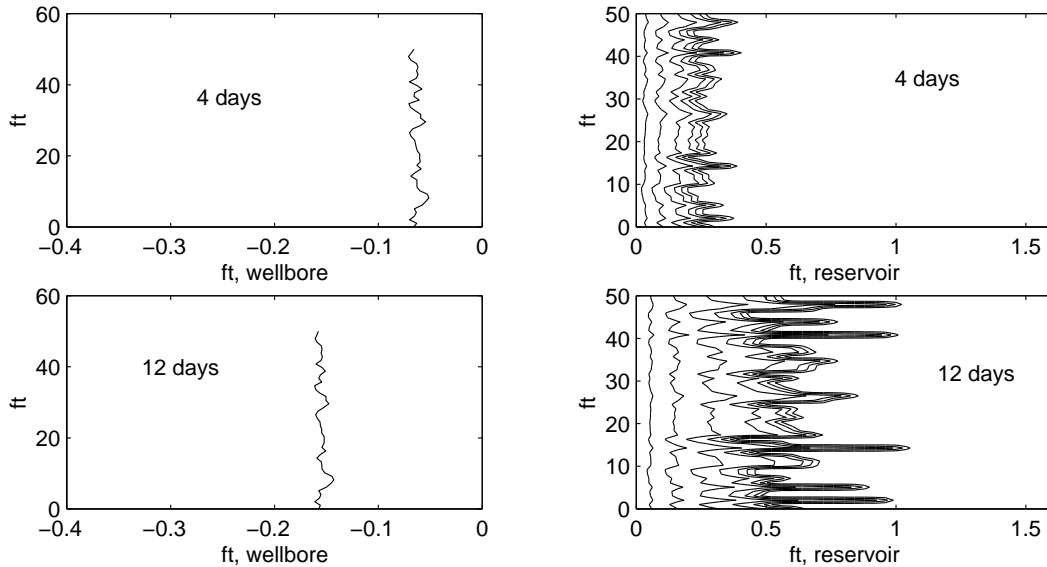


FIG. 3.1. Cross section of the reservoir. Left figures show the motion of the mudcake at different times. Right figures show the invasion of the reservoir with the base (in our case, water) of the mud. Right of the most right curve on the right figures is pure oil, while other contour lines show the mixture of oil and water.

#### 4. Conclusions and work in progress

To model the dynamic of the mudcake at large times the effects of the shear stresses due to vertical circulation of the mud is needed to be taken into account. The growth of the mud cake ceases when the shear stresses become equal to the yield stresses of the mud. This process is often called the erosion of the mud. After this time the only changes occur in the filtration area as the water (or oil) of the mud filtrate into the reservoir. Note that in the case of oil based mud the final established thickness of the mud (the thickness at large times) is smaller than in the case of water based muds because the viscosity of the oil is greater than water, and hence the shear stresses produced by the vertical motion of the mud is greater in the case of oil based muds.

To take roughly into account the effects of the shear stresses in our model we can do the following. Given the flux of the mud  $Q$  in the vertical direction we can compute the average velocity of the mud at each vertical point using the incompressibility of the mud. The average velocity at each point  $z$  is equal to

$$v_z(z) = \frac{Q}{d(z)}$$

where  $d(z)$  is the width at point  $z$  (see Fig. 4.1). Further assuming that the mud cake wall is almost impermeable (no slip boundary condition, this assumption is used for large times in [1]) we can calculate the shear stresses at each time instant as

$$\tau = \frac{d}{dx} v_z(z) = v_z(z)/d(z).$$

Further when this shear stress is equal to the yield stress of the mudcake we stop the growth

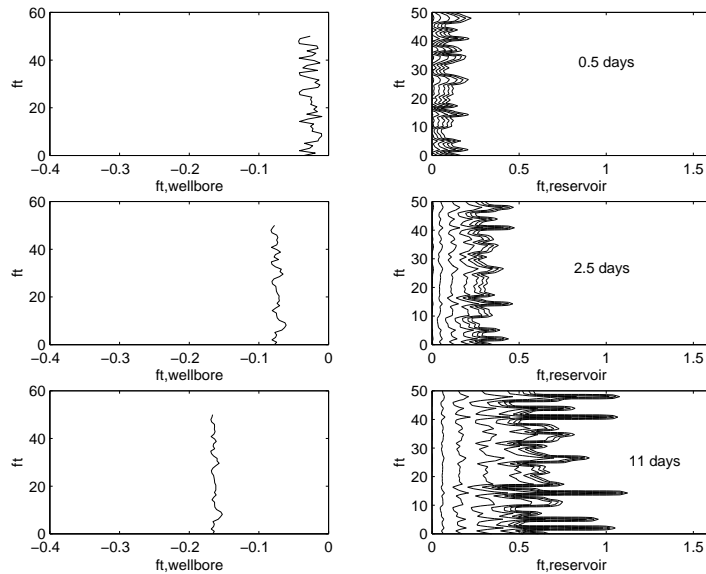


FIG. 3.2. *Cross section of the reservoir. Left figures show the motion of the mudcake at different times. Right figures show the invasion of the reservoir with the base (in our case, water) of the mud. Right of the most right curve on the right figures is pure oil, while other contour lines show the mixture of oil and water.*

of the mudcake at this location  $z$ .

The effects of the mudcake compaction also can be taken into account. Because of the compaction of the mudcake the permeability of the mudcake decreases dramatically. To incorporate this effect into our model we need to specify the permeability of the mudcake as a function depending on the pressure,  $k(p)$ . As the pressure increases the permeability of the mudcake decreases. This can be easily incorporated into the code provided  $k(p)$ .

Next step is to model accurately the motion of the mud in the wellbore. It is believed that the most liquid drilling muds are non-Newtonian plastic fluids. For plastic fluids a certain value of stress (yield stress) must be exceeded in order to initiate movement. This can be numerically modeled using finite element or finite volume methods and shear stresses can be accurately calculated. This is the problem currently I am working on.

### Acknowledgements.

I am grateful to Professor Fadil Santosa for introducing me to this problem.

### REFERENCES

- [1] Wilson Chin. *Formation invasion :with applications to measurement-while-drilling, time lapse analysis, and formation damage*. Houston : Gulf Pub. Co., 1995.

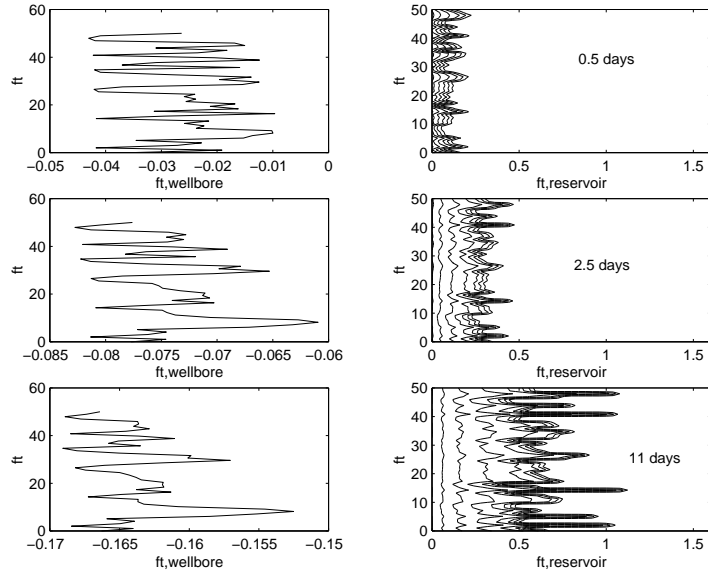


FIG. 3.3. The same as Fig. 3.2 in a limited distance interval to show the presence of the heterogeneity in the mudcake front.

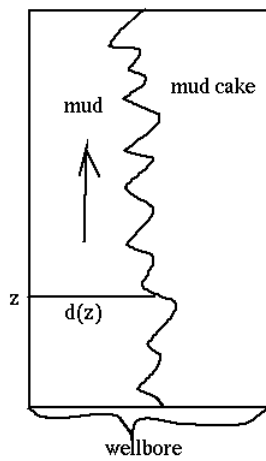


FIG. 4.1. A schematic plot of the shear flow